

Comparative study of wear resistance of Plasma sprayed Commercial and Crushed Alumina Coatings

Pritam Das

*Assistant Professor, Department of Mechanical Engineering
Saroj Mohan Institute of Technology, Guptipara, West Bengal, India*

Abstract- Two types of alumina powder, namely commercial agglomerated alumina and crushed alumina have been plasma sprayed to form coatings. These coatings have been studied for their microstructure, phases, porosity, hardness and wear resistance. The wear resistances of the coatings have been assessed using ball on disc method. The coatings have shown good wear resistance. The commercial agglomerated alumina has undergone adhesive wear and microfracturing, whereas for the crushed alumina coating both abrasion and microfracturing wear modes were active. The crushed alumina has shown a better wear resistance.

Key Words:- Plasma spray, Commercial Alumina, Agglomerated Alumina, Microfracturing

I. INTRODUCTION

Thermal spray processing has become a very important coating technology. New and further developments in plasma spray processes spray devices, and spray materials has led to advantages in the realization of functional coatings and applications ranging from conventional to highly specialized industries. The plasma-spray process can be regarded as almost universal because of its inherently high-process temperature, which allows almost unlimited combinations of coating and base material to be used. Coating technology has become one of the most innovative found in a modern economy. The outstanding advantage is that by using advanced coating materials and by varying coating and substrate materials, many surface problems can be solved, thus saving and conserving rare and expensive materials in production, maintenance, and repair in any engineering field. Using this process, the desired coating material, in powder form, is fed into a gas plasma stream. This plasma is created by striking an electrical arc between a finger type tungsten cathode and a nozzle-type copper anode inside the plasma torch. The injected powder particles get melted, highly accelerated, and catapulted to the substrate, forming the desired lamellar structured coating. Different plasma-spraying process variants allow their working with all kinds of materials, from low-melting temperature plastics to high-melting-temperature metals and ceramics. The high working temperature of the spray gases, which is reached by the plasma process and the automation of plasma-spray devices, makes it possible to achieve high-quality coatings for a wide variety of applications.

Ceramic materials such as alumina, zirconia, titania, chromia, silica and yttria have been used widely as surface coating materials to improve wear, erosion, cavitations, fretting and corrosion resistance. They are especially useful in applications where wear and corrosion resistances are required simultaneously. Plasma sprayed ceramic coatings such as alumina coatings have been widely applied to structural materials and various machine parts in order to improve resistances to wear, corrosion, oxidization, erosion, and heat. The present study aims to explore the tribological aspects of plasma sprayed alumina coatings of commercial and crushed powders.

Experimental Procedure explained in section II. Experimental results are presented in section III. Concluding remarks are given in section IV.

II. EXPERIMENTAL PROCEDURE

2.1. Introduction

This chapter deals with the details of the experimental procedures followed in this study. The coating procedure itself requires some basic preparation, i.e., grit blasting followed by cleaning. Then plasma spraying has been

conducted for the generation of isolated splats and processing of bulk coatings as well. After plasma spraying, the test sample have been subjected to a series of tests, e.g., microscopy of cross sections of the coatings, microhardness measurement, porosity measurement, X-ray diffraction studies, etc. On the other hand, the coatings have been characterized for their morphology, cross section, wear resistance using Pin-On-Disc tribometer, etc. Each procedure is documented in this chapter.

2.2. Processing of the coating

2.2.1. Powders for Coating

In this work, two different Aluminium Oxide top coats and nickel based standard bond coats have been used for the generation of coating. The particulars of the powders have been listed in Table 2.1. The powders have been characterized using a JEOL JSM 5800 Scanning Electron Microscope and a Phillips X-ray diffractometer (PW 1729 generator and PW 1710 goniometer).

2.2.2. Preparation of Substrates

C 20 low carbon steel substrates have been chosen for the experiment. The substrates have been grit blasted inside a suction type grit blasting cabinet (Sandstorm, Bangalore, India) using alumina grits of grit size 24, 100 psi air pressure and 100 mm standoff distance. The grit blasted samples have been cleaned ultrasonically. Coating has been done immediately after cleaning.

Table: 2.1. Powders used in coating

Name	Size	Composition	Morphology	Manufacturer
Nickel Aluminium	+45 μm – 90 μm	Ni 95 wt% Al 5 wt%	Clad	M/S Sulzer Metco, USA (150 NS)
Commercial Alumina	+45 μm – 90 μm	Al ₂ O ₃ 99.443 wt% TiO ₂ 0.007 wt% SiO ₂ 0.045 wt% Na ₂ O 0.280 wt% CaO 0.025 wt% Fe ₂ O ₃ 0.200 wt%	Agglomerated	M/S Hindalco, India (HT)
Crushed Alumina	+30 μm - 45 μm	98 – 99 % α -Al ₂ O ₃	Crushed and bulky	M/S Sulzer Metco, USA (450 NS)

2.3. Experimental Details

Low Carbon Steel of rectangular size (130×25×6) has been taken as the substrate material for this study. The initial size of the specimens is 130×25×6 mm. The 25 mm wide sides have been ground using a surface grinder, so as to make them parallel. The ground specimens have been grit blasted using a suction type grit blasting cabinet and alumina grits of grit size 24. The other grit blasting parameters are the following: blasting pressure 100 psi, standoff distance 100 mm, blasting angle 90°. After grit blasting, the sample has been put in the ultrasonic bath for 5 minutes and thermal spraying has followed immediately.

Atmospheric Plasma spraying has been done using a 3MB silver metco plasma spraying facility. The parameters used for coating given in Table 2.2. Alumina powders have been supplied from M/S Hindalco, India (HT) and M/S Sulzer Metco (Metco-105NS) company.

Table: 2.2 Plasma spray parameters

1	Stand of distance (SOD) (mm)	150
2	Nozzle diameter (mm)	7 mm
3	Arc current (A)	500 A
4	Arc voltage (V)	65 V
5	Powder injection angle	90°
6	Secondary gas (hydrogen) flow rate (slpm)	10
7	Primary gas (nitrogen) flow rate (slpm)	80
8	Powder flow rate (kg/hr)	1.5
9	Substrate material	C20 steel
10	Preheating of the substrate (°C)	200

The rectangular specimens have been sliced to 25 × 25 size. The cross sections of the slices have been polished using a LABOPOL semi-automatic polisher. Abrasive papers of grit size 220, 400, 600, 800, 1000 and 1600 have been used during wet polishing. Thereafter polishing has been undertaken diamond pastes containing diamond particles of sizes 8, 6, 4, 3 and 1 μ. The cross sections have been observed using Olympus optical microscope and ZEISS EVO 60 SEM. The microhardness of the samples has been measured using LECO microhardness tester, equipped with a Vickers's indenter. The normal load has been kept at 100 g. The porosity has been measured using IMAGEJ image processing software and the results are in acceptable range.

2.4.Procedure for wear Experiment

The coatings were characterized for their wear performance along with the wear testing parameters, are listed in Table 2.3. For all coatings bearing steel ball served as rubbing counterparts.

Table: 2.3 wear test parameters

Sliding Distance (m)	100
Normal Load (kg)	2.0, 3.0 & 5.0
Sliding Velocity (mm/sec)	104.6, 157 & 209.33
Rubbing Counterpart	6.35 mm diameter bearing steel ball, TiN coated

The Wear experiment has been undertaken using a DUCOM pin and disc wear tester fig 2.1

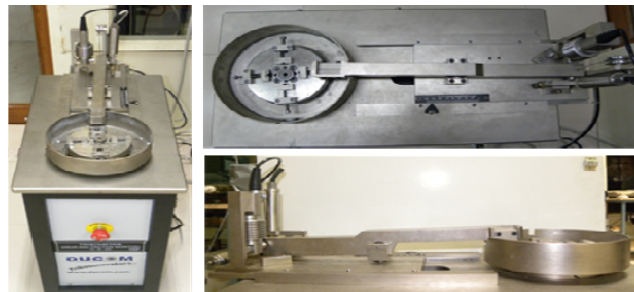


Figure 2.1 Photographs of Tribometer

In this device, the sample is held horizontally on a turn table and is rotated at a preset speed. At the same time the rubbing counterpart is held on special holder and is pressed on to the sample under a normal load. The normal load is applied by means of standard weights. Wear is measured by measuring the loss of weight of the coating with the help of weighing machine, AG 135, METTLER TOLEDO. Each trial has been repeated for three times and the average is reported. In some cases the loss of weight of the ball has also been recorded. For understanding the wear mechanisms, the wear tracks have been observed under the SEM (ZEISS EVO 60) using various magnifications ranging from $500\times$ to $5000\times$.

III. RESULTS AND DISCUSSION

3.1. Introduction

This chapter deals with the primary characteristics of the all the powders used in this study and those of the coatings produced. This includes the morphology of all the powders, the phases of the alumina based powders, the cross sectional features of the coatings, the phases of the coatings and wear resistance of the coatings.

3.2. General Characteristics of Powders

Figures 3.1 (a) show the Ni-5wt% Al bond coat powders. This powder is clad in nature Figure 3.2 (a) is the secondary electron image of the agglomerated commercial alumina powders. The sizes of the agglomerates are in the range of $45 - 90 \mu\text{m}$. The corresponding X-ray diffraction is shown in Figure 3.2 (b). The peaks are from α phase. Figures 4.3 (a) and (b) show the morphology of the as-received crushed alumina powder and the corresponding X-ray diffraction, respectively. This powder has been produced by crushing and grinding and hence it has a chunky morphology.

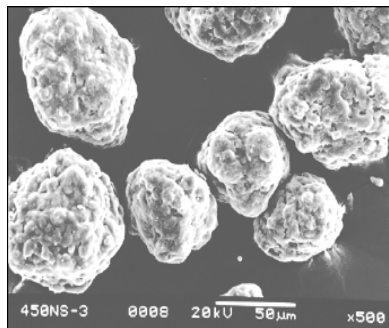


Figure 3.1. Secondary Electron Images of Ni-5 wt% Al

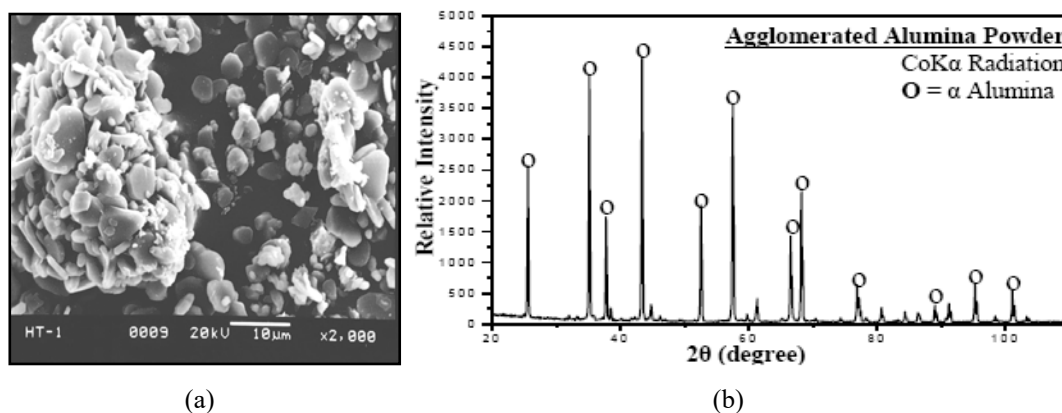
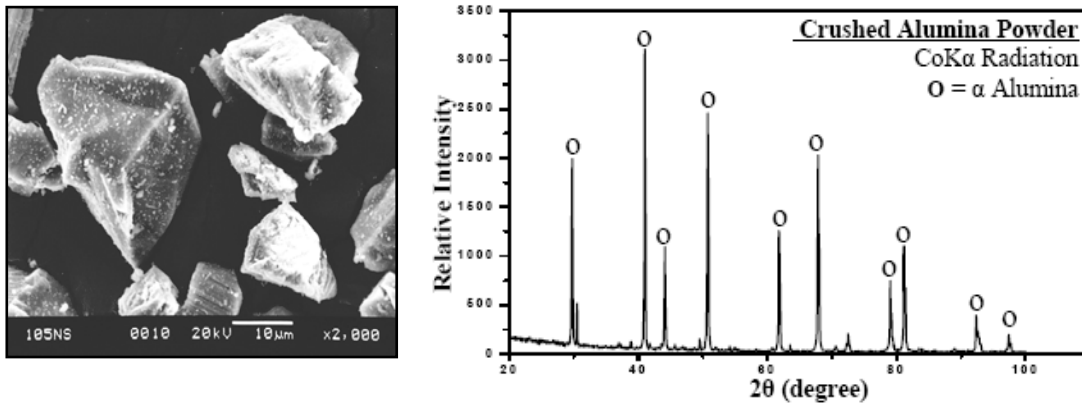


Figure 3.2 (a) Secondary Electron Image of the Agglomerated Alumina and (b) XRD pattern of the same

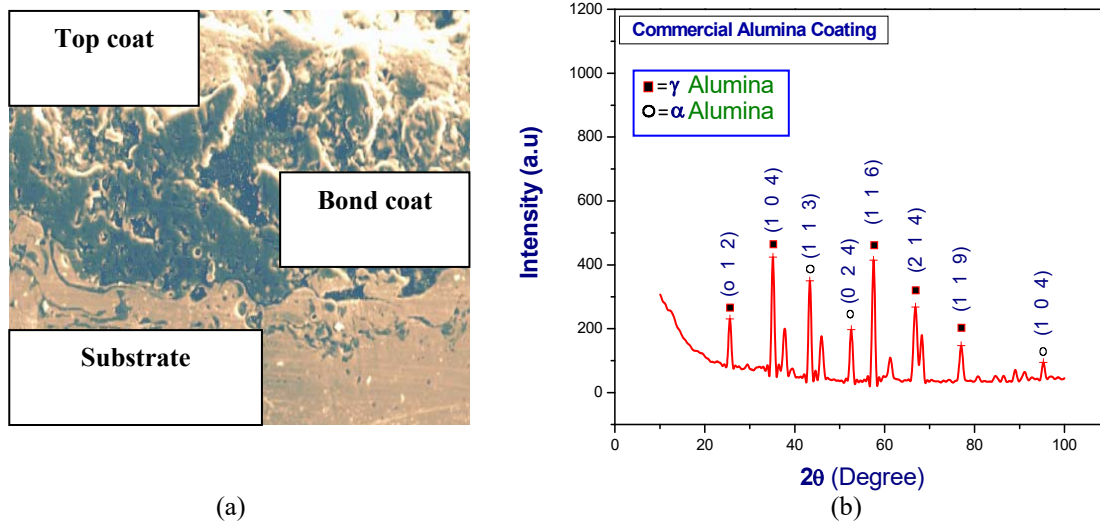


(a) (b)
Figure 3.3 (a) Secondary Electron Image of the Crushed Alumina and (b) XRD pattern of the same

3.3. General Features of the Coatings

The general morphology of the coatings in cross section and the corresponding X-ray diffractions are shown in Figures 3.4 – 3.5. Figure 3.4 (a) is a secondary electron image of the polished cross section of the agglomerated commercial alumina coating. The bond coat and the substrate layer can also be seen in this figure. The coating is well adherent with the bond coat, does not contain too many pores and in general shows good microstructural integrity. The accompanying (Figure 3.4 (b)) X-ray diffraction pattern shows peaks from metastable γ phase in addition to quite a few sharp and tall α peak. This is not entirely unexpected of this powder, since it is made up of smaller sub particles. Some of these smaller particles do not undergo melting and they act as α nuclei from which α phase grown in the coating. It may be noted in this context that in general, α to γ transformation occurs during plasma spraying of α alumina powders. The hardness and porosity of this coating is 1150 Hv and 11 %, respectively.

Figure 3.5 (a) is the optical micrographs of the polished crushed alumina coating in cross section. The three layers of the coating, top coat, bond coat and the substrate are well visible. This coating also shows low porosity and well adherent interfaces. Unlike agglomerated commercial alumina, no significant clubbing of unmelted or semi molten particles has been detected in the microstructure of this coating. In contrast to Figure 3.5 (b) here the γ peaks are very prominent. So this powder appears to have a better melting characteristic as compared to commercial agglomerated alumina. The hardness and porosity of this coating is 990 Hv and 7.2 %, respectively.



(a) (b)
Figure 3.4 (a) Secondary Electron Images of the Polished Agglomerated Alumina Coating in Cross Section and (b) XRD Pattern of the Same.

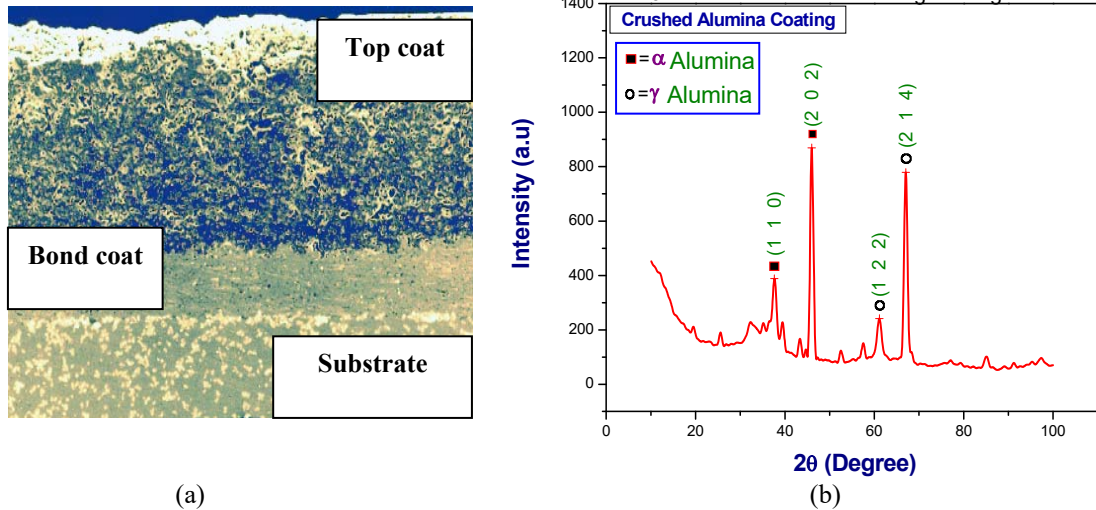


Figure 3.5 (a) Secondary Electron Images of the Polished Crushed Alumina Coating in Cross Section and (b) XRD Pattern of the Same.

Plasma sprayed coatings are made up of small molten particles and these particles cannot occupy the entire coating volume during spraying. This results in porosity. The porosity obtained for these two coatings is within acceptable limits. A slightly higher porosity of the agglomerated powder coating is attributed to the presence of unmelted particles. These particles are dislodged during polishing and one obtains a slightly inflated porosity value for such coatings.

3.4 Coating wear

3.4.1 Commercial agglomerated alumina

The mass loss in wear of the commercial agglomerated alumina coating under various speed/load conditions is shown in Figure 3.6. Wear has been found to increase with rise in both speed and load. This is typical of adhesive wear. At higher speed and load, more energy is injected into the small contact area, causing greater wear. The wear mechanism has been confirmed by studying the worn surface under the SEM.

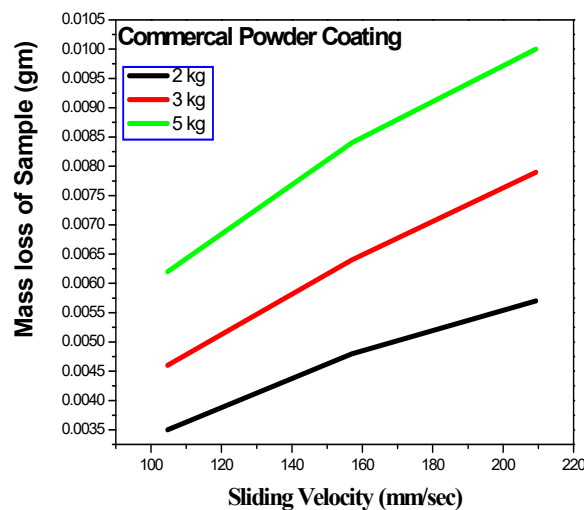
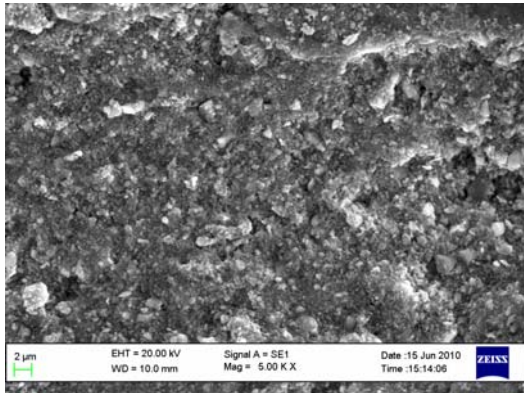


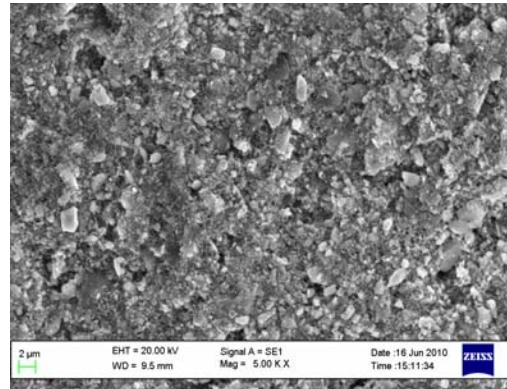
Figure 3.6 Mass loss of commercial alumina powder coating

Figure 3.7 (a) shows the secondary electron image of the commercial agglomerated alumina coating obtained with a load of 2 kg and a sliding velocity of 157 mm/s. The coating does not feature any polishing marks of abrasion. It has

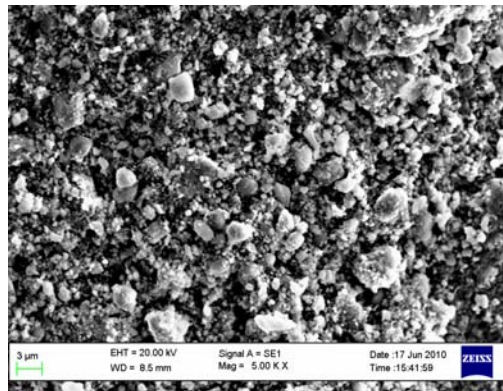
undergone adhesive wear and compaction. Similar features have been observed for a slightly higher load of 3 kg (Figure 3.7 (b)). However, while the load is increased to 5 kg (Figure 3.7 (c)) the coating has undergone pulverization. This is attributed to the micro fracturing of the coating under higher load. The fractured particles are easily removed from the contact area. So as a whole at a higher load mass loss increases. It appears that for this material wear progresses by the combined effect of adhesive wear and micro fracturing.



(a) 2kg, 157 mm/sec



(b) 3kg, 157 mm/sec



(c) 5kg, 157 mm/sec

Figure 3.7 shows the secondary electron image of the commercial agglomerated alumina coating at different magnifications

3.4.2 Crushed alumina

Figure 3.8 shows the wear characteristics of crushed alumina under various speed load conditions. Here also wear increases with both speed and load. However, the extent of mass loss in this case is less than that of agglomerated alumina. The wear mechanism is interpreted from the secondary electron images shown in Figure 3.9.

Figure 3.9 (a) shows the worn surface subjected to load of 2 kg and sliding velocity of 157 mm/s. Here the polishing marks on the worn surface are indicative of abrasive wear. This in turn is attributed to the roughness of the ball surface at the contact area. The hard coating has also abraded on the ball and marks of abrasion are visible on the ball surface (Figure 3.9. (e)). This roughened ball surface has abraded on the coating. With a further increase of the load part of the coating has been found to flake off (Figure 3.9 (b)). This is known as delamination. Similar wear

mechanism has prevailed with further increase in load and speed (figure 3.9 (c)). In places crushing of the coating has also been observed (Figure 3.9(d)). Crushing, i.e., microfracturing occurs in those spots where the powder has not been well melted and the coating is not cohesive enough. As a whole it appears that this coating undergoes wear by abrasion and microfracturing.

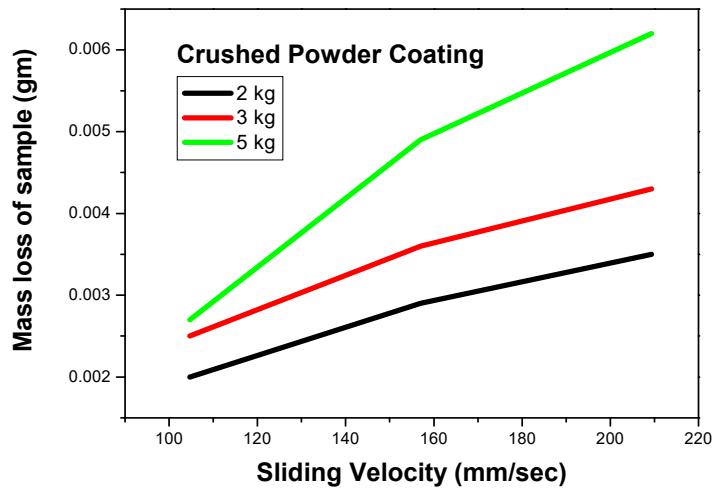
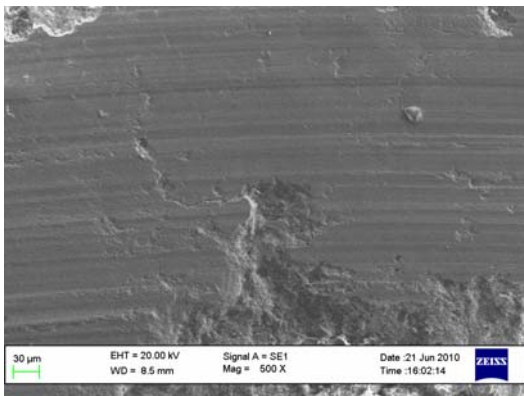
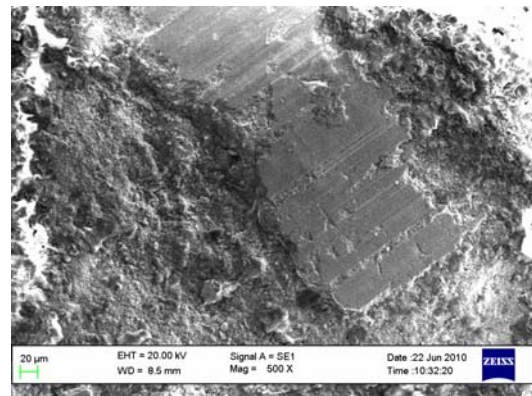


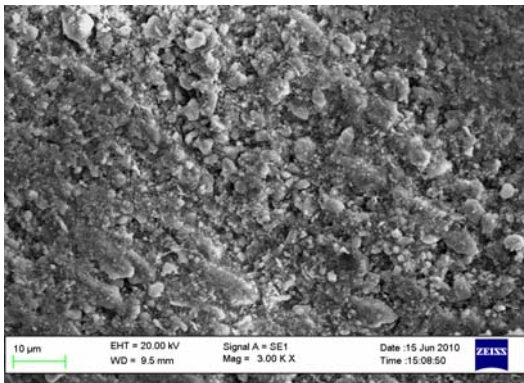
Figure 3.8 Mass loss of Agglomerated Alumina powder coating



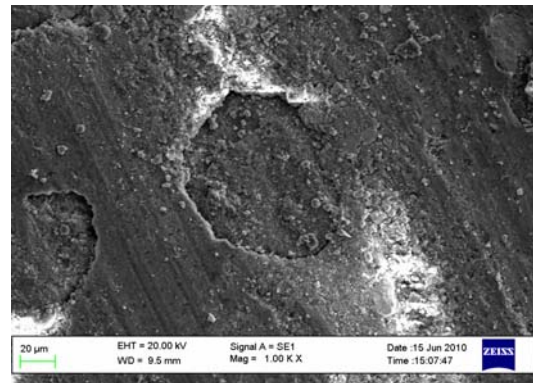
(a) 2 kg, 157 mm/sec



(b) 3 kg, 157 mm/sec



(c) 5 kg, 157 mm/sec



(d) 5 kg, 157 mm/sec



(e) Ball 5 kg

Figure 3.9 shows the secondary electron image of the crushed alumina coating at different magnifications and at different load and the image of the TiN coated ball undergone wear using 5kg load

IV. CONCLUSIONS

Commercial agglomerated alumina and crushed alumina powders have been plasma sprayed to obtain hard coating with acceptable porosity. The coatings show good microstructural integrity. In the agglomerated alumina both α and γ phases were present. In the crushed alumina coating γ was the major phase. The agglomerated alumina coating contained a fraction of unmelted particles which promotes nucleation of α alumina in the coatings. Both coating show good wear resistance under ball on disc testing condition. The commercial alumina failed by adhesive mode along with microfracturing. For the crushed alumina two wear modes were active, namely, abrasive and microfracturing.

REFERENCES

- [1] T.Z.Kattamis, M.Chen, R.Hui, J.Kelly, C. Fountzoulous and M.Levy, 1995, *J. Adhesion Science and Technology*, v 9(5), p 907.
- [2] Gell, M., Jordan, E. H., Sohn, Y. H., Goberman, D., Shaw, L., Xiao, T. D. (2001), Development and implementation of plasma sprayed nanostructured ceramic coatings, *Surface and Coatings Technology*, Vol. 146–147, pp. 48–54.
- [3] Westergard, R., Erickson, L.C., Axe, N., Hawthorne, H. M., Hogmark, S. (1998), The erosion and abrasion characteristics of alumina coatings plasma sprayed under different spraying conditions, *Tribology International*, Vol. 31, No. 5, pp. 271–279.
- [4] Zhao, L., Seemann, K., Fischer, A., Lugscheider, E. (2003), Study on atmospheric plasma spraying of Al_2O_3 using on-line particle monitoring, *Surface and Coatings Technology*, Vol. 168, No. 2–3, pp. 186–190.
- [5] H. Mindivan, C. Tekmen, B. Dikici, Y. Tsunekawa and M. Gavali, “Wear behavior of plasma sprayed composite coatings with in-situ formed Al_2O_3 ”, *Materials and Design*, 2009.
- [6] Wang, D., Tian, Z., Shen, L., Liu, Z., Huang, Y. (2009), Microstructural characteristics and formation mechanism of Al_2O_3 –13 wt.% TiO_2 coatings plasma-sprayed with nanostructured agglomerated powders, *Surface & Coatings Technology*, Vol. 203, No. 10–11, pp. 1298–1303.
- [7] Pantelis, D. I., Psyllaki, P., Alexo-poulos, N. (2000), Tribological behaviour of plasma-sprayed Al_2O_3 coatings under severe wear conditions, *Wear*, Vol. 237, No. 2, pp. 197–204.
- [8] Sarikaya, O. (2005), Effect of some parameters on microstructure and hardness of alumina coatings prepared by the air plasma spraying process, *Surface and Coatings Technology*, Vol. 190, No. 2–3, pp. 388–393.
- [9] Guessasma, S., Bounazef, M., Coddet, C. (2004), Note on POD test parameters to study wear behaviour of alumina–titania coatings, *Materials Characterization*, Vol. 52, No. 3, pp. 237–241.
- [10] McPherson, R. (1973), The structure of Al_2O_3 - Cr_2O_3 powders condensed from a plasma, *Journal of Materials Science*, Vol. 8, No. 6, pp. 859–862.
- [11] McPherson, R. (1980), On the formation of thermally sprayed alumina coatings, *Journal of Materials Science*, Vol.15, No. 12, pp. 3141–3149.
- [12] Guessasma, S., Bounazef, M., Nardin, P., Sahraoui, T. (2006), Wear behavior of alumina–titania coatings: analysis of process and parameters, *Ceramics International*, Vol. 32, No. 1, pp. 13–19.
- [13] Devasenapathi, A., Ang, C.B., Yu, S.C.M., Ng, H.W.(2001), Role of particle injection velocity on coating microstructure of plasma sprayed alumina–validation of process chart, *Surface and Coatings Technology*, Vol. 139, No. 1, pp. 44–54.
- [14] Wang, D., Tian, Z., Shen, L., Liu, Z., Huang, Y. (2009), Microstructural characteristics and formation mechanism of Al_2O_3 –13 wt.% TiO_2 coatings plasma-sprayed with nanostructured agglomerated powders, *Surface & Coatings Technology*, Vol. 203, No. 10–11, pp. 1298–1303.
- [15] S. Das, P.P. Bandyopadhyay, S. Ghosh, T.K. Bandyopadhyay, and A.B. Chattopadhyay, “Processing and Characterization of Plasma-Sprayed Ceramic Coatings on Steel Substrate: Part II. On Coating Performance” September 1, 2003
- [16] S. Das, P.P. Bandyopadhyay, T.K. Bandyopadhyay, S. Ghosh, and A.B. Chattopadhyay , “Processing and Characterization of Plasma-Sprayed Ceramic Coatings on Steel Substrate: Part I. On Coating Characteristics”